AD-A117 632 NAVAL UNDERWATER SYSTEMS CENTER NEW LONDON CT NEW LO--ETC F/G 17/1
DETECTION THRESHOLD CALCULATIONS FOR CROSS CORRELATION PROCESSI--ETC(U)
MAR 80 P N MIKHALEVSKY

UNCLASSIFIED NUSC-TM-801040 NL

END
DATE
FILMED
8 82
DTIC

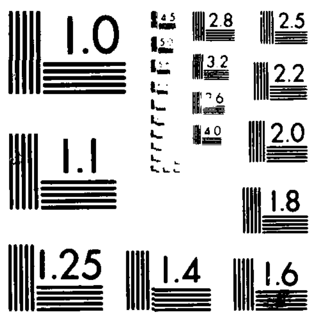

MICROCOPY RESOLUTION TEST CHART
NATIONAL BUREAU OF STANDARDS 1963-A

AD A117632

TM No.
801040

NAVAL UNDERWATER SYSTEMS CENTER
NEW LONDON LABORATORY
NEW LONDON, CONNECTICUT 06320

Technical Memorandum

DETECTION THRESHOLD CALCULATIONS

FOR

CROSS CORRELATION PROCESSING

Date: 18 March 1980

Author: PETER N. MIKHALEVSKY
Advanced Systems Technology Div.
Special Projects Department

Approved for public release;distribution unlimited

30 Jan1981

ROUTING SHEET
FOR RELEASE OF UNCLASSIFIED TECHNICAL INFORMATION

TITLE OF PROPOSED RELEASE "Detection Threshold Calculations For Cross Correlation Processing" by LT P. Mikhalevsky

DATE 18 Mar 1980

TYPE OF INFORMATION (ABSTRACT, PAPER, REPORT, PRESS RELEASE, ETC.)
NUSC Tech Memo #801040

INTENDED FOR PUBLICATION IN/PRESENTATION AT
Cleared for availability to scientific community

BRIEF STATEMENT OF PURPOSE OF RELEASE

TO THE BEST OF YOUR KNOWLEDGE, IS PROPOSED RELEASE:	ORIGINATOR YES	ORIGINATOR NO	TECHNICAL REVIEWER YES	TECHNICAL REVIEWER NO	DEPARTMENT HEAD YES	DEPARTMENT HEAD NO	SECURITY YES	SECURITY NO
1. TECHNICALLY ACCURATE?	✓		✓		✓			
2. FREE OF INFORMATION WITH POTENTIAL INTELLIGENCE VALUE?	✓		✓		✓			
3. FREE OF INFORMATION WHICH WOULD ADVERSELY AFFECT THE SECURITY OF THE U.S.?	✓		✓		✓		✓	
4. CONSIDERED BORDERLINE FROM BEING CLASSIFIED?		✓		✓		✓		
5. [illegible] PREVIOUS RELEASE?		✓		✓				
6. LIABLE TO DAMAGE THE SUCCESS OF OPERATION OF A SYSTEM?		✓		✓		✓		
7. SECURITY CLASSIFICATION GUIDES HAVE BEEN CHECKED TO ENSURE NO CLASSIFIED OR "FOR OFFICIAL USE ONLY" INFORMATION IS CONTAINED IN THIS RELEASE.	✓						✓	

ROUTING		SIGNATURE	REMARKS
1. ORIGINATOR (NAME) LT P. Mikhalevsky	335M	P. Mikhalevsky	
2. TECHNICAL REVIEWER (NAME) G. C. Carter	3331	D Griffith GCC	UNCLASSIFIED
3. DEPARTMENT HEAD (NAME) D. Walters	33	David Walters	
4. SECURITY (NAME) (NB2/LB3) P. Beskin	034		
5. PUBLIC AFFAIRS (NAME) B. LaCoe	033		~~Requires~~ DIST STATEMENT "B" D.ST. STATEMENT "A" Applies
6. OFFICER IN CHARGE (NAME) LCDR L. Gorham	03		☑ APPROVED ☐ DISAPPROVED DATE:

Approved for public release; distribution unlimited

3ND-NUSC-5216/1 (REV. 8-70)

NEW LONDON LABORATORY
NAVAL UNDERWATER SYSTEMS CENTER
NEW LONDON, CONNECTICUT 06320

AREA CODE 203
442-0771
AUTOVON 636 + EXT.
IN REPLY REFER TO:

313:PNM:aab
Ser: 0313-122
10 June 1980

From: P.N. Mikhalevsky
To: Distribution

Ref: (a) P.N. Mikhalevsky, "Detection Threshold Calculations for Cross Correlation Processing", NUSC TM No. 801040, dated 18 March 1980

1. Please make the following corrections to reference (a). Equation (14) page 13 should read:

$$MAL = \frac{1}{B} \int_{f_1}^{f_2} \exp\left[-2\alpha_A(f,R)\right] df$$

and on page 14, in Figure 2 the loss values should be reduced by a factor of 2 so that the curves represent .5, 1.5, 4.5, and 7.5 dB of loss.

P.N. MIKHALEVSKY

DTIC COPY INSPECTED 2

Accession For
NTIS GRA&I
DTIC TAB
Unannounced
Justification
Distribution/
Availability Codes
Avail and/or
Special
A

TM No.
801040

ABSTRACT

Detection threshold calculations are performed for cross correlation processing of the received signals from two fixed omnidirectional sensors of a moving source generating an arbitrary random power spectrum. The effects of doppler decorrelation and volumetric absorption, and the degradation as a result of multiple bottom bounce and surface reflections are included. The equations for ROC curves are presented. A computer program which accepts as input the source power spectrum, noise power spectrum, averaging time, frequency analysis band, and sensor baseline separation solves for the detection threshold given a .5 probability of detection and .001 probability of false alarm.

ADMINISTRATIVE INFORMATION

This memorandum was prepared under Project No. A69050, "Broadband Cross Correlation Processing", Program Manager CDR V. Simmons DARPA: NUSC Principle Investigator G. Mayer, Code 313.

The author of this memorandum is located at the New London Laboratory of the Naval Underwater Systems Center, New London, Connecticut 06320.

NOTATION

B	Analysis bandwidth $\equiv f_2 - f_1$
b	Sensor base line
c	Speed of sound in water
f_2	Upper frequency limit for analysis
f_1	Lower frequency limit for analysis
$h(t)$	Impulse response function accounting for volumetric absorption, surface, and/or bottom reflections(s)
k	Equals 0 (no target), or 1 (target present)
$n_i(t)$	Noise at receiver i ($i=1,2$)
$H(f)$	Transfer function of $h(t)$
$N_i(t)$	Noise spectrum
$s(t)$	Source function
$G_s(f)$	Source power spectral density
R	Range from target to midpoint of sensor baseline
T	Averaging time
v	Target speed
f, x_1, x_2, x_3, x_4, t	Variables of integration
v_i	Target speed along the line of sound between target and receiver i ($i=1,2$)
$x_{Ri}(t)$	Received signal at receiver $i(i=1,2)$
$\alpha_A(f,r)$	Volumetric absorption loss coefficient, function of frequency and range
a_i	Time compression or expansion at receiver i ($i=1,2$) $\equiv 1+v_1/c$

P_D	Probability of detection
P_F	Probability of false alarm
Erf(x)	Error function $\equiv (2/\sqrt{\pi}) \int_0^x e^{-t^2} dt$
σ_0^2	Variance of the correlator output given no target $\equiv \mathrm{Var}\{y\|k=0\}$
σ_1^2	Variance of the correlator output given the target is present $\equiv \mathrm{Var}\{y\|k=1\}$
m_1	Expected value of the correlator output given the target is present $\equiv E\{y\|k=1\}$
y	Correlator output
DT	Detection threshold
NL	Noise level
SL	Source level
SE	Signal Excess
TL	Transmission Loss

TM No.
801040

INTRODUCTION

Detection threshold calculations are performed for cross correlation processing of two received signals each having propagated via no, one or many bottom bounces and/or surface reflections from a moving source generating an arbitrary random power spectrum. The two receiving sensors are omnidirectional, fixed and of arbitrary baseline separation. A binary hypothesis test is performed and the detection threshold computed for a probability of detection of .5 and a probability of false alarm of .001.

The effects of doppler and absorption on the mean correlator output are investigated. It is shown that in general degradation due to doppler will be $\gtrsim$3dB when $BT \gtrsim (c/V)(R/b)\{1+1/4\ (^{b}/_{R})^{2}\}^{\frac{1}{2}}$. This can only be considered a rough guide, however, as the doppler degradation is a function not only of analysis bandwidth but upper and lower cut off frequencies. The detection threshold curves in fact exhibit high peaks corresponding to nulls in the correlator output as a function of range as a result of this dependence. For an analysis band of 300 Hz it is shown that absorption is $\lesssim$3dB for ranges $\lesssim$30km and/or frequencies $\lesssim$600 Hz.

Bottom losses are taken from measured values in the abyssal plains south of Bermuda and extrapolation based upon other measurements. Surface interactions are characterized by the Kirchoff approximation assuming a random Gaussian surface, though computations of detection threshold for surface bounce paths are not performed. The purpose of this report, however, is not to characterize surface and bottom interactions but how to account for their effects in cross correlation processing given specific conditions and assumptions.

ANALYSIS

In general we have two received signals

$$x_{R1}(t) = ks(\alpha_1 t) * w(t) * h(t) + n_1(t) * w(t) \tag{1}$$

$$x_{R2}(t) = ks(\alpha_2 t) * w(t) * h(t) + n_2(t) * w(t) \tag{2}$$

where s(t) is the source function, $n_i(t)$ is the noise at receiver i, h(t) is the impulse response function accounting for volumetric absorption, surface and/or bottom reflection(s), w(t) is a weighting function corresponding to a band pass filter in the frequency domain, and k = 0 when no target is present and k = 1 where the target is present. The * denotes convolution.

$$\alpha_1 = 1 + v_1/c \quad \text{and}, \tag{3}$$

$$\alpha_2 = 1 + v_2/c \tag{4}$$

where v_i is the target speed along the line of sound at sensor i. The effect of doppler is thus a time compression or expansion as indicated in Eqs. (1) and (2). It is also assumed that s(t), $n_1(t)$, and $n_2(t)$ are zero mean, uncorrelated, Gaussian, and stationary.

The maximum output of the correlator occurs when x_{R1} is shifted in time by the appropriate time delay relative to x_{R2} which assuming this has been accomplished we can write as,

$$y = \frac{1}{T} \int_{-T/2}^{T/2} x_{R1}(t)\, x_{R2}(t) \; dt \tag{5}$$

For TB large, independent of the distributions of x_{R1} and x_{R2}, y will be a Gaussian random variable, thus knowledge of the mean and variance of y is

all that is required to completely characterize the probabilistic behavior of y.

A. <u>The Expected Value of y</u>

The expected value of y given k recalling the above assumptions is

$$E[y|k] = \frac{1}{T}\int_{-T/2}^{T/2} k^2 E\{[s(\alpha_1 t)*w(t)*h(t)][s(\alpha_2 t)*w(t)*h(t)]\}\,dt \tag{6}$$

If we perform the indicated convolutions and write the correlation function of s(t) as the inverse of its power spectral density $G_s(f)$ we obtain,

$$E[y|k] = \frac{k^2}{T}\int_{-T/2}^{T/2} dt \int_{-\infty}^{\infty} dx_1 \int_{-\infty}^{\infty} dx_2 \int_{-\infty}^{\infty} dx_3 \int_{-\infty}^{\infty} dx_4 \int_{-\infty}^{\infty} df$$
$$\cdot\; G_s(f)\, e^{i2\pi f(\alpha_1 t - \alpha_1 x_1 - \alpha_1 x_3 - \alpha_2 t + \alpha_2 x_2 + \alpha_2 x_4)} \tag{7}$$
$$\cdot\; w(x_1)w(x_2)h(x_3)h(x_4)$$

Integrating over the x_i's we have

$$E[y|k] = \frac{k^2}{T}\int_{-T/2}^{T/2} dt \int_{-\infty}^{\infty} df \;\; G_s(f)\, e^{i2\pi f(\alpha_1 t - \alpha_2 t)} \tag{8}$$
$$\cdot\; W(\alpha_1 f)W^*(\alpha_2 f)H(\alpha_1 f)H^*(\alpha_2 f)$$

where H(f) is the transfer function accounting for bottom and surface interactions and volumetric absorption and W(f) is a band pass filter with a gain of $1/\sqrt{2B}$ for $-f_2<f<-f_1$ and $f_1<f<f_2$ and zero elsewhere. Interchanging the order of integration and integrating over t we have,

$$E[y|k] = k^2\int_{-\infty}^{\infty} \operatorname{sinc}[\pi f T(\alpha_1-\alpha_2)]\, G_s(f) \tag{9}$$
$$\cdot\; W(\alpha_1 f)W^*(\alpha_2 f)H(\alpha_1 f)H^*(\alpha_2 f)\,df$$

For $\left| f_2 \frac{V_1}{c} \right| \ll B$ and $\left| f_2 \frac{V_2}{c} \right| \ll B$ we can write,

$$E[y|k] \cong \frac{k^2}{B} \int_{f_1}^{f_2} G_s(f)\,\mathrm{sinc}\left[\pi f T(\alpha_1 - \alpha_2)\right] \left| H(f) \right|^2 df \tag{10}$$

where $\mathrm{sinc}(x) \equiv \frac{\sin(x)}{x}$.

This is as far as we can proceed without knowledge of $G_s(f)$ and $H(f)$. One can readily see from Eq. (10) that the effect of doppler is a sinc function weighting of the source spectrum. The sinc function has its first zero crossing at

$$f_o = \left[T(\alpha_1 - \alpha_2)\right]^{-1} \tag{11}$$

If the center of the analysis band is near or greater than f_o and $B \gtrsim f_o$ severe degradation (>>3DB) of the correlator output can be expected. If we choose a "worst case" geometry, namely the target is travelling an a course parallel to the sensor baseline and crossing the perpendicular bisector of the baseline, then the condition $B \gtrsim f_o$ can be written as

$$BT \gtrsim (c/V)(R/b)\left[1 + \frac{1}{4}(b/R)^2\right]^{\frac{1}{2}} \tag{12}$$

As a representative case the loss in the mean due to doppler is plotted in Fig. 1, assuming the source spectrum is flat and the analysis band extends from 0 to B Hz. Eq. (10) is used neglecting the bottom transfer function.

For bottom or surface bounce paths doppler degradation will not be as severe as for direct path propagation as the target speed V is reduced by the factor $\cos\theta$ where θ is the bottom or surface grazing angle. Furthermore though it is true that the doppler degradation will be more severe as the range is

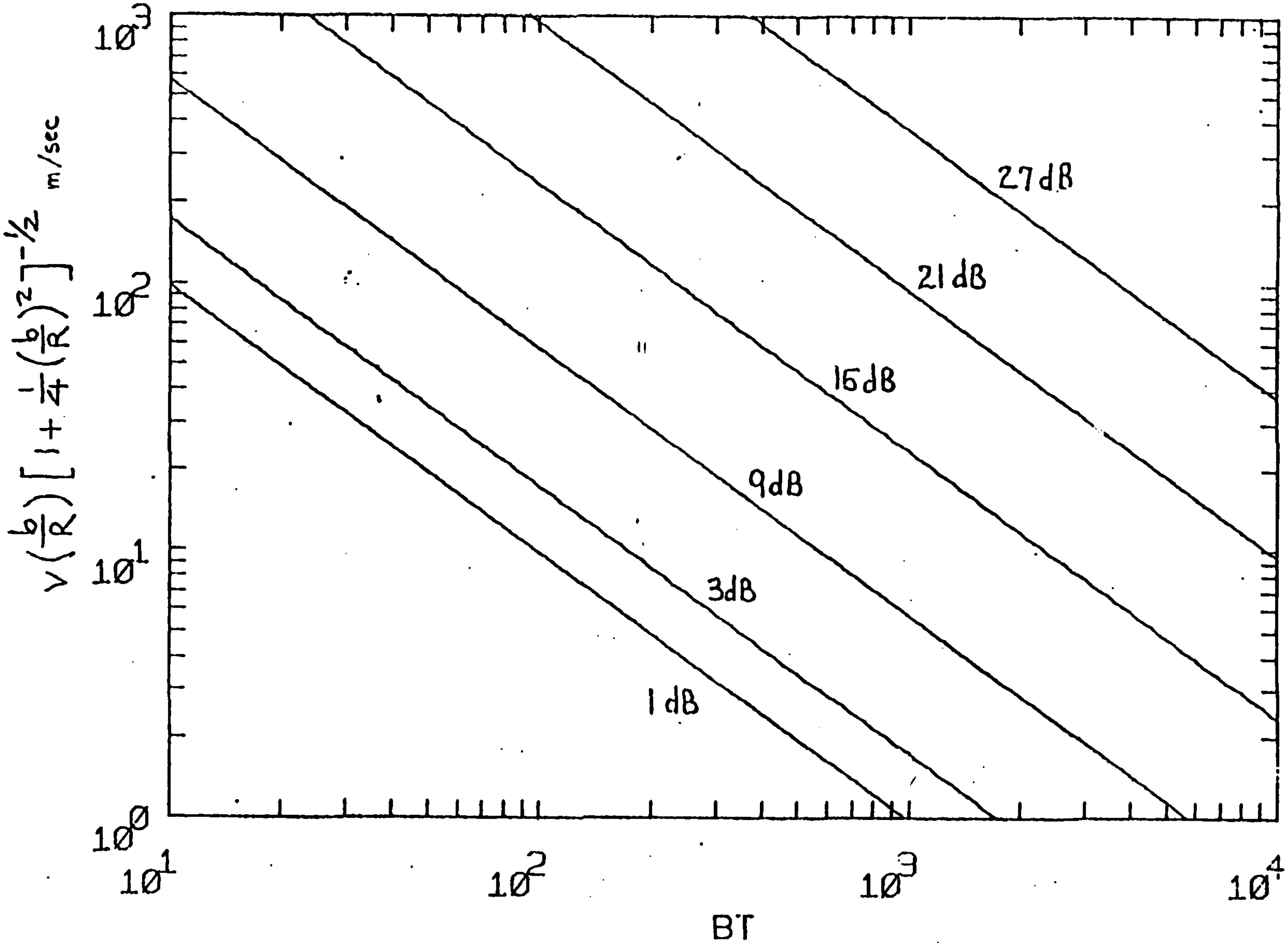

Fig. 1 Mean loss due to doppler decorrelation for a target on course parallel to the sensor baseline, b, crossing the perpendicular bisector at range R, with speed V (m/sec) with an analysis band from 0 to B Hz and averaging time T.

reduced, the signal is experiencing less transmission loss which can reduce or negate this effect. More discussion on this will be given in Section E. However, because the sinc function does go negative it is possible to obtain zero output if the analysis band is appropriately placed relative to the main and/or side lobes of the sinc function. Because the zero crossings of the sinc function will change as the range to the target changes (relative doppler between sensors is a function of range) nulls in mean correlator output and therefore corresponding spikes in detection threshold appear as functions of range (see Section E.)

Assuming no surface and bottom interactions we can express H(f) as

$$H(f) = \exp\left[-\alpha_A(f,R)\right] \tag{13}$$

where $\alpha_A(f,R)$ is the absorption loss coefficient which is a function of frequency and range (see for example ref. (1)). If we apply Eq. (13) to Eq. (10), assume a flat source spectrum and no doppler we have,

$$MAL = \frac{1}{B}\int_{f_1}^{f_2} \exp\left[-\alpha_A(f,R)\right] df \tag{14}$$

for the Mean Absorption Loss. Note that this quantity is range dependent. Eq. (14) is plotted in Fig. 2 with B=300 Hz for low frequency cutoff f_1 vs. range R.

B. <u>The Variance of y</u>

The expected value of y^2 given k is

$$E\left[y^2|k\right] = \frac{1}{T^2}\int_{-T/2}^{T/2}\int_{-T/2}^{T/2} E\left[x_{R1}(t_1)x_{R2}(t_1)x_{R1}(t_2)x_{R2}(t_2)\right] dt_1\, dt_2 \tag{15}$$

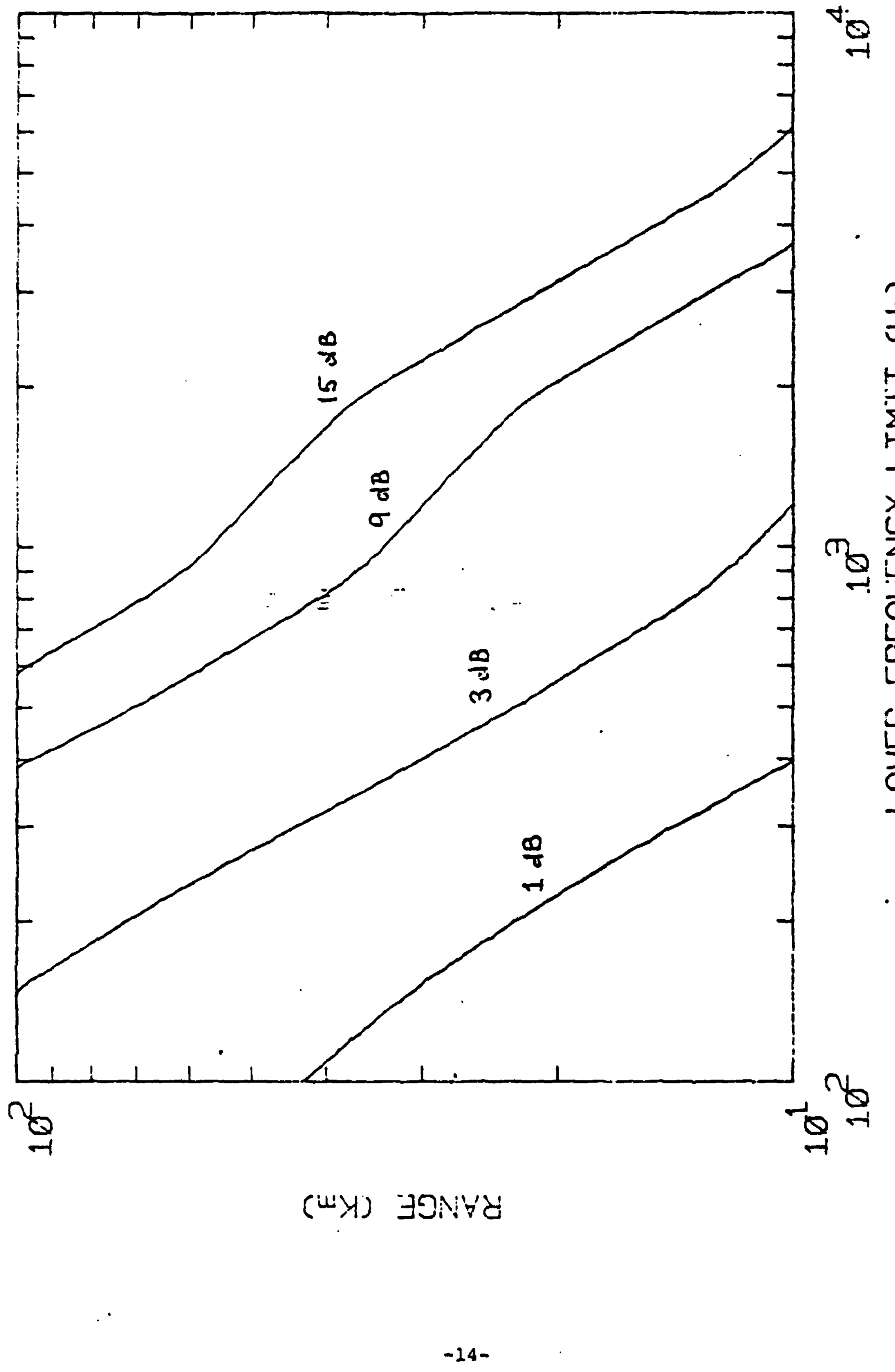

Fig. 2. Mean loss due to volumetric absorption for an analysis bandwidth of 300 Hz.

Exploiting the Gaussian assumption we moment factor Eq. (15),

$$E[y^2|k] = \frac{1}{T^2}\int_{-T/2}^{T/2}\int_{-T/2}^{T/2}\Big\{E[x_{R1}(t_1)x_{R2}(t_1)]E[x_{R1}(t_2)x_{R2}(t_2)] \tag{16}$$

$$+ E[x_{R1}(t_1)x_{R1}(t_2)]E[x_{R2}(t_1)x_{R2}(t_2)]$$

$$+ E[x_{R1}(t_1)x_{R2}(t_2)]E[x_{R2}(t_1)x_{R1}(t_2)]\Big\}\,dt_1\,dt_2$$

Thus the variance of y is

$$\mathrm{Var}[y|k] = \frac{1}{T^2}\int_{-T/2}^{T/2}\int_{-T/2}^{T/2}\Big\{E[x_{R1}(t_1)x_{R1}(t_2)]E[x_{R2}(t_1)x_{R2}(t_2)] \tag{17}$$

$$+ E[x_{R1}(t_1)x_{R2}(t_2)]E[x_{R2}(t_1)x_{R1}(t_2)]\Big\}\,dt_1\,dt_2$$

Applying Eqs. (1) and (2) in Eq. (17), performing the indicated convolutions, transforms, and changing the double integration over t_1 and t_2 to a single integration over $\tau=t_1-t_2$ where possible we have,

$$\mathrm{Var}[y|k] = \frac{1}{T}\int_{-T}^{T}\left(1-\frac{|\tau|}{T}\right)\Big\{ⒶⒷ + ⒺⒷ + ⒻⒶ + ⒺⒻ\Big\}\,d\tau \tag{18}$$

$$+ \frac{1}{T^2}\int_{-T/2}^{T/2}\int_{-T/2}^{T/2} ⒸⒹ \; dt_1\,dt_2$$

where

$$Ⓐ \simeq \frac{k^2}{B}\int_{f_1}^{f_2} G_s(f)\cos(2\pi f\alpha_1\tau)\,|H(f)|^2\,df$$

$$Ⓑ = \frac{k^2}{B}\int_{f_1}^{f_2} G_s(f)\cos(2\pi f\alpha_2\tau)\,|H(f)|^2\,df$$

$$Ⓒ \simeq \frac{k^2}{B}\int_{f_1}^{f_2} G_s(f)\cos[2\pi f(\alpha_1 t_1-\alpha_2 t_2)]\,|H(f)|^2\,df$$

$$\text{Ⓓ} \simeq \frac{k^2}{B}\int_{f_1}^{f_2} G_s(f)\cos\left[2\pi f(\alpha_2 t_1 - \alpha_1 t_2)\right]|H(f)|^2\,df$$

$$\text{Ⓔ} \simeq \frac{1}{B}\int_{f_1}^{f_2} G_{n_1}(f)\cos(2\pi f\tau)\,df$$

$$\text{Ⓕ} \simeq \frac{1}{B}\int_{f_1}^{f_2} G_{n_2}(f)\cos(2\pi f\tau)\,df$$

The approximations arise as a result of the assumptions that $\left|f_2\frac{V_1}{C}\right| \ll B$ and $\left|f_2\frac{V_2}{C}\right| \ll B$.

C. Binary Hypotheses Test

We recall that for $TB \gg 1$ the correlator output y is a Gaussian random process when the target is present ($k=1$) or not ($k=0$). Applying a binary hypothesis test we obtain

$$Erf^{-1}(1-2P_D) = \frac{\sigma_0}{\sigma_1}Erf^{-1}(1-2P_F) - \frac{m_1}{\sqrt{2}\,\sigma_1} \tag{19}$$

where $Erf^{-1}(x)$ is the inverse error function, $\sigma_0^2 \equiv Var\{y|k=0\}$, $\sigma_I^2 \equiv Var\{y|k=1\}$, $m_1 \equiv E\{y|k=1\}$, P_D is the probability of detection, and P_F is the probability of false alarm. Eqs. (10), (18), and (19) define the Receiver Operating Characteristics for cross correlation processing. With $P_D=.5$, and $P_F=.001$ we obtain from Eq. (19),

$$m_1 = \sigma_0\sqrt{2}\,Erf^{-1}(.998) = \sigma_0(3.09\ldots) \tag{20}$$

where,

$$m_1 = \frac{1}{B}\int_{f_1}^{f_2} G_s^-(f)\,\mathrm{sinc}\left[\pi f T(\alpha_1-\alpha_2)\right]|H(f)|^2\,df \tag{21}$$

where $G_s^-(f)$ is the source expectrum attenuated equally by frequency such that

Eq. (20) is satisfied, and

$$\sigma_o^2 = \frac{1}{B^2 T}\int_{-T}^{T}\left(1-\frac{|\tau|}{T}\right)\int_{f_1}^{f_2}\int_{f_1}^{f_2} G_{n_1}(f)\, G_{n_2}(v) \cos(2\pi f \tau) \cos(2\pi v \tau)\, df\, dv\, d\tau \quad (22)$$

If we assume equal noise at the receivers and exploit the fact that TB>>1,

$$\sigma_o^2 \cong \frac{1}{4B^2 T}\int_{-\infty}^{\infty}\left[\int_{-\infty}^{\infty} G_n(f)\, H_W(f)\, e^{i2\pi f \tau} df\right]^2 d\tau \quad (23)$$

where $H_w(f)$ is a passband filter of gain 1 for $|f_1|<f<|f_2|$. Noting that the inner integral is the transform of $R_n(\tau)$, the correlation function of the noise, convolved with $h_w(\tau)$, and then applying Parseval's theorem we have simply,

$$\sigma_o^2 \cong \frac{1}{2TB^2}\int_{f_1}^{f_2}\left[G_n(f)\right]^2 df \quad (24)$$

If we assume a flat signal ($G_s(f)=S$) and noise ($G_n(f)=N$) spectrums, no doppler, bottom, surface, or volumetric losses and combine Eqs.(20), (21) and (24) we have

$$R_{SN} = \frac{1}{\sqrt{TB}}\, Erf^{-1}(.998) \quad (25)$$

where R_{SN} is the signal to noise ratio ($\equiv S/N$). This result was first obtained by Nuttall [2].

D. <u>The Transfer Function H(f)</u>

In general for multiple bottom and surface reflections we have

$$H(f) = \prod_{i=1}^{N}\prod_{j=1}^{M} H_{B_i}(f)\, H_{S_j}(f)\, e^{-\alpha_A(f,R_T)} \quad (26)$$

for N bottom and M surface reflections. The exponential term accounts for volumetric absorption and R_T is the total range including the bounces. Furthermore, the H_B's and H_S's are in reality average filter responses, averaged over the time and/or spacially varying surface as the bottom and sea surfaces are random surfaces. These realities in fact limit the applicability of the

of the analysis in Section B, particularly the moment factoring used to derive the variance, which requires essentially that the result of the convolution of s(t), a Gaussian random process, with h(t) the impulse response, also be a Gaussian random process. Note that independent of the nature of H(f), the correlator output will always be Gaussian for TB>>1.

If we assume the reflecting surface is random with displacement $\zeta(x,t)$ and employ the Kirchoff approximation we can write {3},

$$\mathcal{H}_{s_j}(f) = \int_{-\infty}^{\infty} p_{\zeta_j}(\zeta_j) \exp\left(-i \frac{2\pi f}{c} \zeta_j \sin\theta_s\right) d\zeta_j \qquad (27)$$

where $p_{\zeta_j}(\zeta_j)$ is the probability density function of the surface for the jth reflection, c is the speed of sound, and θ_s is the surface grazing angle. Assuming a Gaussian surface we have,

$$\mathcal{H}_{s_j}(f) = \exp\left[-\left(\frac{2\pi f}{c}\right)^2 \sigma_{\zeta_j}^2 \sin^2\theta_s\right] \qquad (28)$$

where $\sigma_{\zeta_j}^2$ is the variance of the surface for the jth reflection. With this characterization, extension to multiple reflections is straightforward.

For a single surface reflection

$$E[y|K] \cong \frac{K^2}{B}\int_{f_1}^{f_2} G_s(f)\,\mathrm{sinc}\left[\pi f T(\alpha_1-\alpha_2)\right] \cdot \exp\left\{-\alpha_A(\alpha_1 f,R)-\alpha_A(\alpha_2 f,R)-2\left[\frac{4\pi^2 f^2\sigma_\zeta^2\sin^2\theta_s}{c^2}(\alpha_1^2+\alpha_2^2)\right]\right\}df \qquad (29)$$

where it is assumed that σ_ζ^2 and θ_s are the same for the surface reflection to each of the two receivers. If we make the further assumption that the two reflection surfaces are separated sufficiently such that they are statistically uncorrelated (with the same variances) computation of the variance of the

correlator outputs is straightforward with similar expressions for $H(\alpha_1 f)H^*(\alpha_2 f)$ in Eq. (18) as given in Eq. (29).

A similar approach can also be applied for bottom reflections. However, when this method was applied predicted and observed bottom losses did not agree, with less bottom loss predicted at low frequencies and more bottom loss predicted at high frequencies than observed. Using measured values {4} for an area south east of Bermuda in which a prototype of the cross correlation processor is operating single bounce losses were extrapolated based on these and other bottom loss measurements {1}. The curves are shown in Fig. 3 for $|H_B(f)|^2$ vs. grazing angle at various frequencies. Clearly surface and bottom interactions must be carefully investigated for the area of operation or else grievous errors could be made in predicting system performance.

E. Calculation of Detection Threshold

A computer program has been developed which accepts as input the target spectrum, target speed, upper and lower frequency limits for the analysis band, and the averaging time, and computes the detection threshold vs. range. The noise spectra are taken from Wenz {5} with three spectra available: heavy noise (shipping density 1, sea state 5), average noise (shipping density .45, sea state 3), and light noise (shipping density 0, sea state 0). Eqs. (20), (21), and (24) are used with numerical integration employing the Romberg Quadrature technique {6} to compute the detection threshold,

$$DT \equiv SL_o - NL \tag{30}$$

where SL_o is the signal level which satisfies Eq. (20), and NL is the noise level.

For broadband signals I define these terms as follows:

$$SL_o \equiv 10 \log_{10} m_1 \tag{31}$$

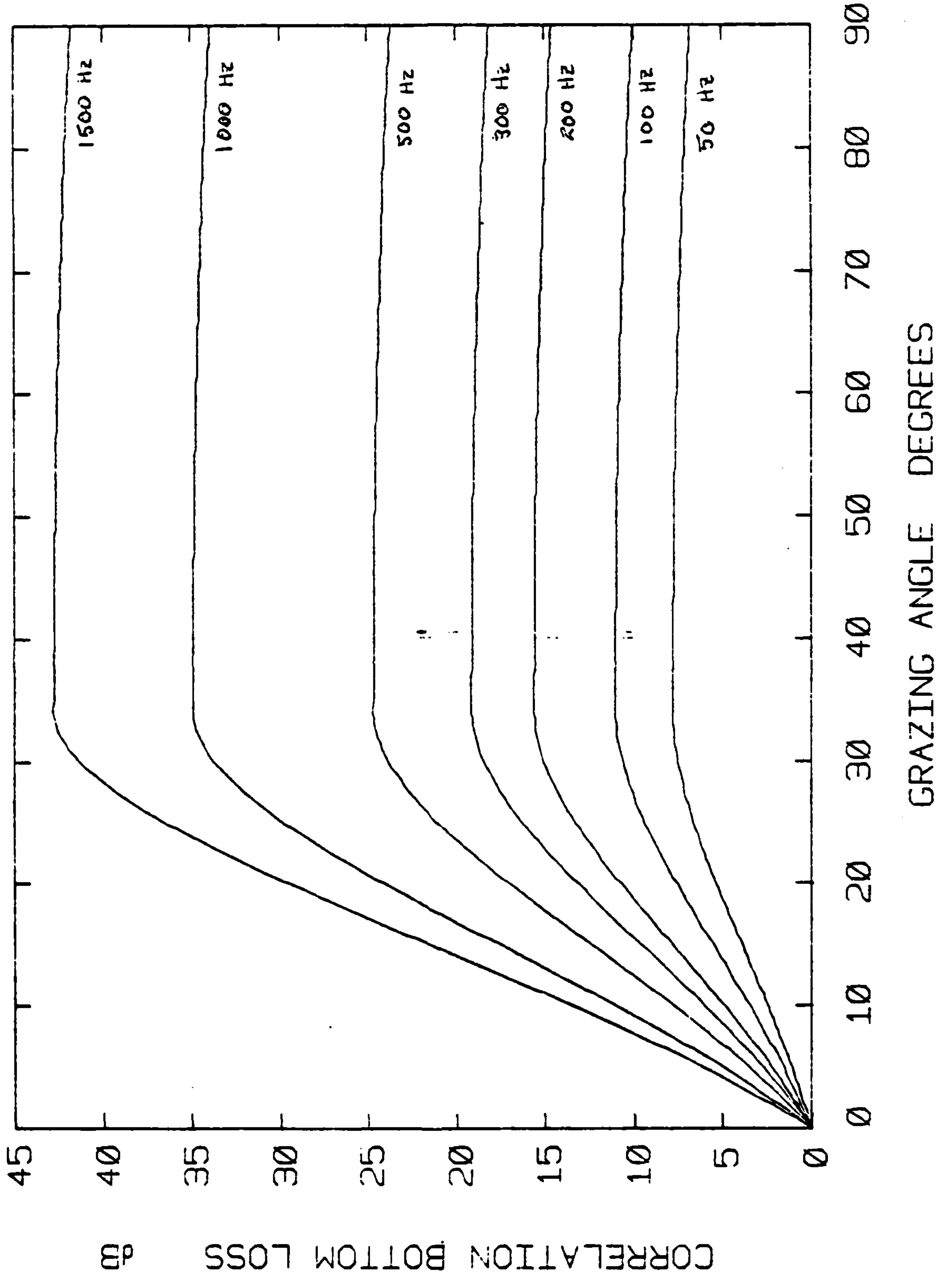

Fig. 3. Bottom loss, $|H_B(f)|^2$, vs. grazing angle.

and

$$NL = \frac{1}{B} \int_{f_1}^{f_2} G_n(f)\,df \qquad (32)$$

Similarly the target source level is defined

$$SL = \frac{1}{B} \int_{f_1}^{f_2} G_s(f)\,df \qquad (33)$$

In Figs. 4-7 are plotted examples of detection threshold and signal excess calculations for the double HX-29 {7} source towed at 15 kts. in average noise conditions assuming a sensor separation of 1.5 km. Signal excess is computed assuming a spherical spreading loss,

$$SE = SL-NL-DT-20 \log_{10}R \qquad (34)$$

The source spectrum is given in Fig. 8. This is the maximum source level for a driving bandwidth of one Hz swept across the frequency band. For broadband operation the source spectrum shape remains the same but must be reduced by $10 \log_{10}B$. The analysis band used in Figs. 4-7 is 150 Hz to 300 Hz with an averaging time of 2.56 secs. Figs. 4 and 5 are the detection threshold and signal excess, respectively, for direct path propagation. Figs. 6 and 7 are the detection threshold and signal excess respectively, for a one bottom bounce path.

Note the detection threshold peak in Fig. 4 which is the result of a corresponding correlator output null due to doppler. For larger analysis bands and longer averaging times there can be many such detection threshold

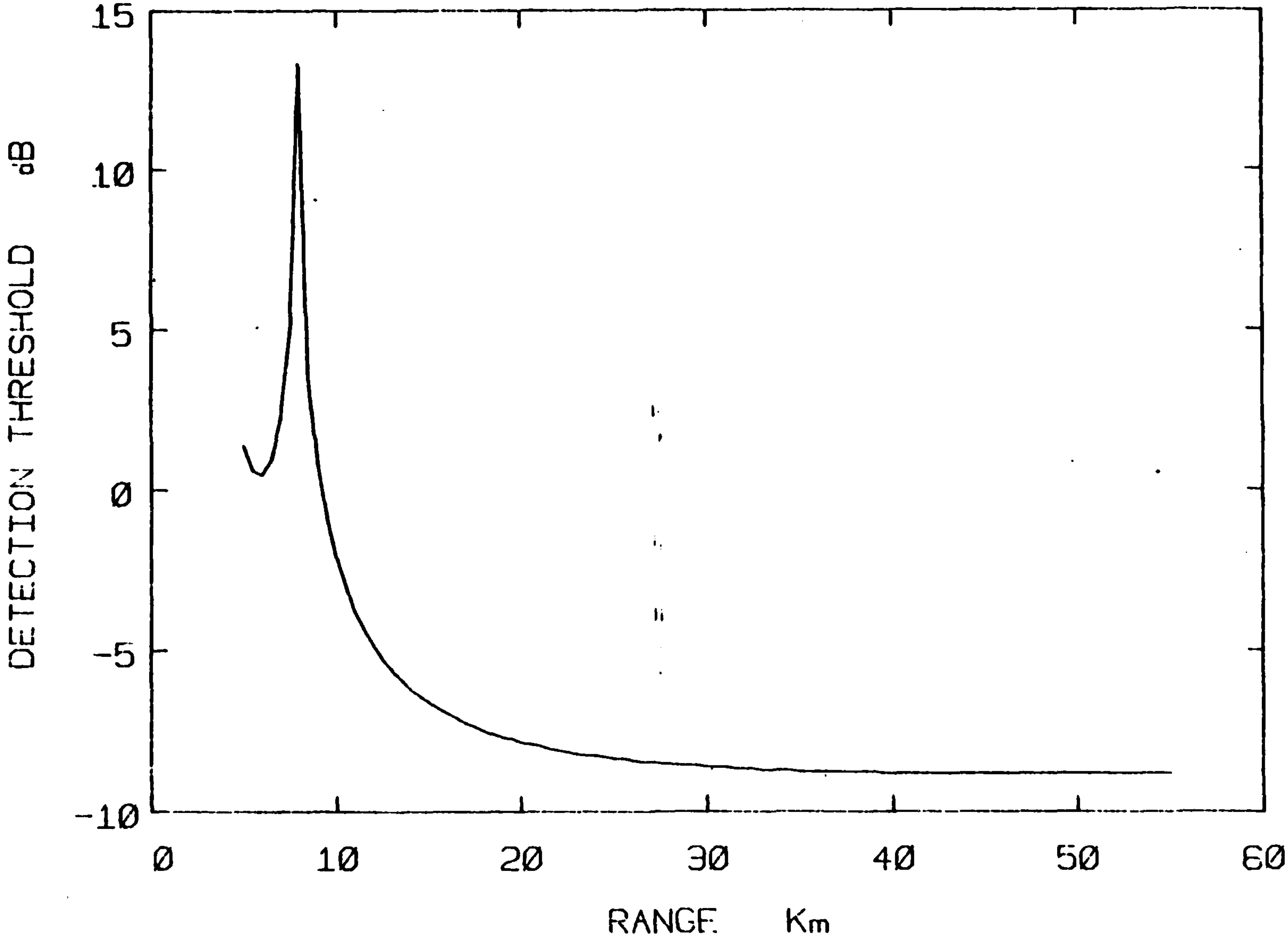

Fig. 4. Detection threshold for the double HX-29 source towed at a speed of 15 kts. assuming direct path propagation.

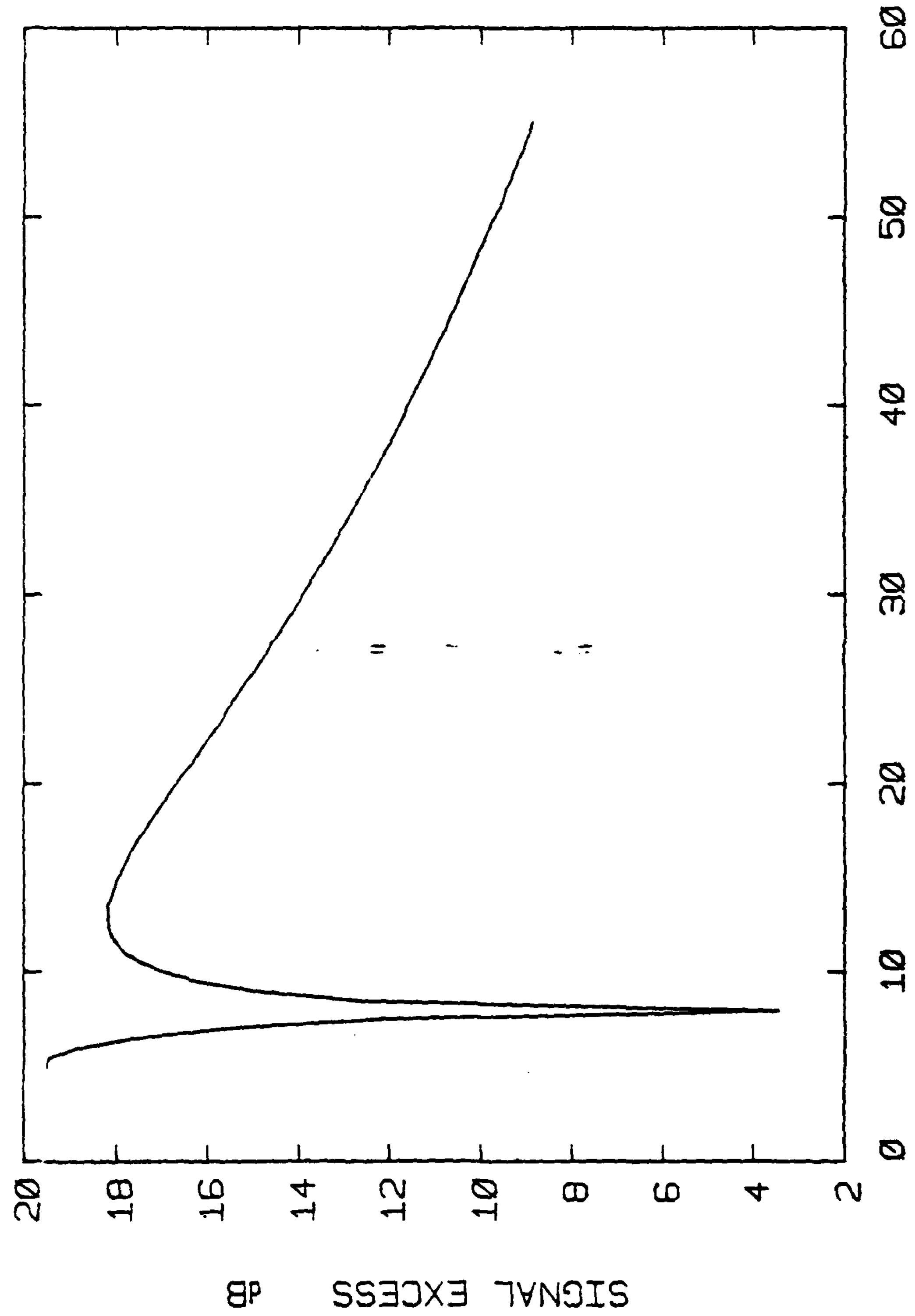

Fig. 5. Signal excess for the case shown in Fig. 4.

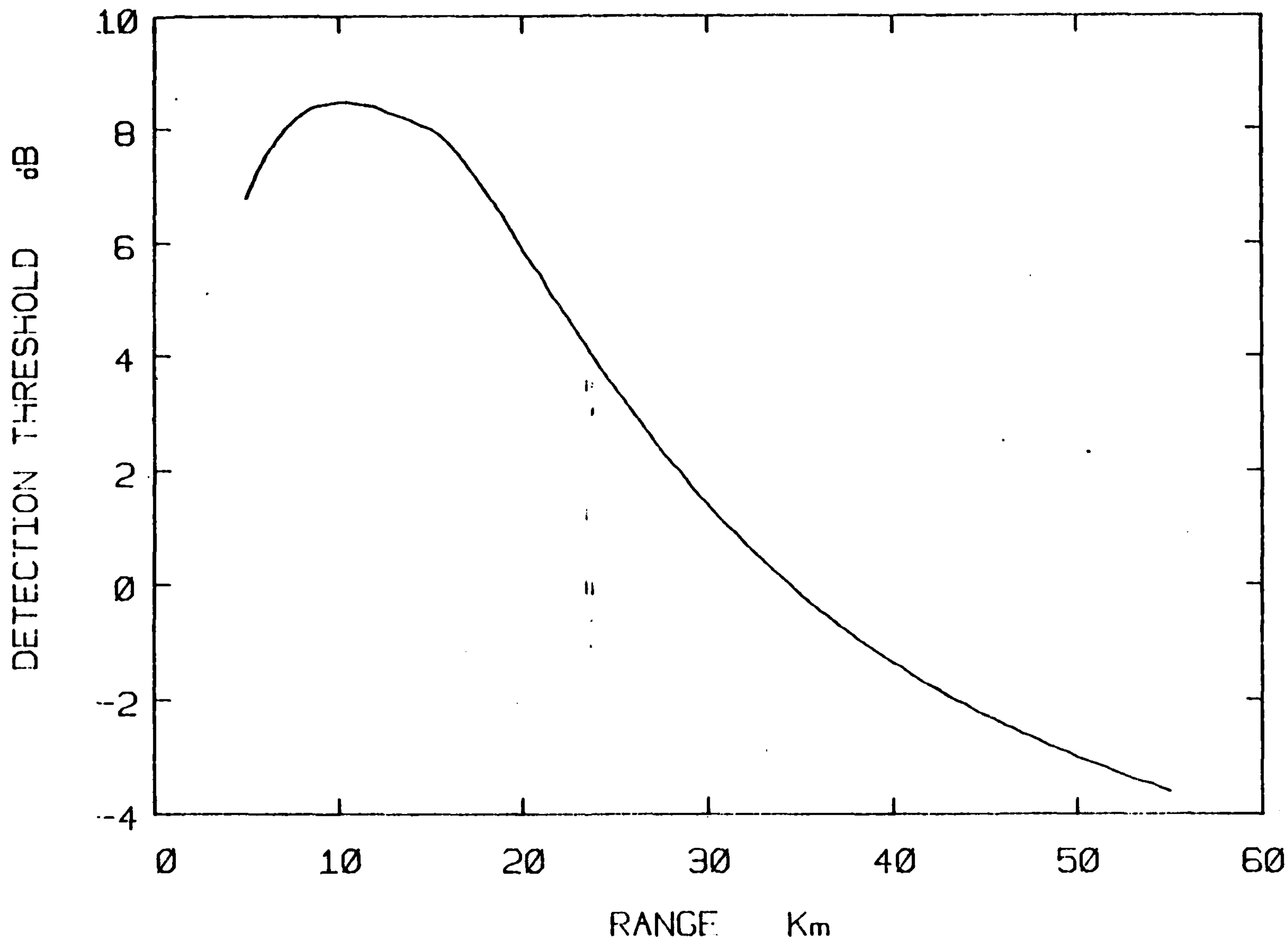

Fig. 6. Detection threshold for the double HX-29 source towed at a speed of 15 kts. assuming a single bottom bounce.

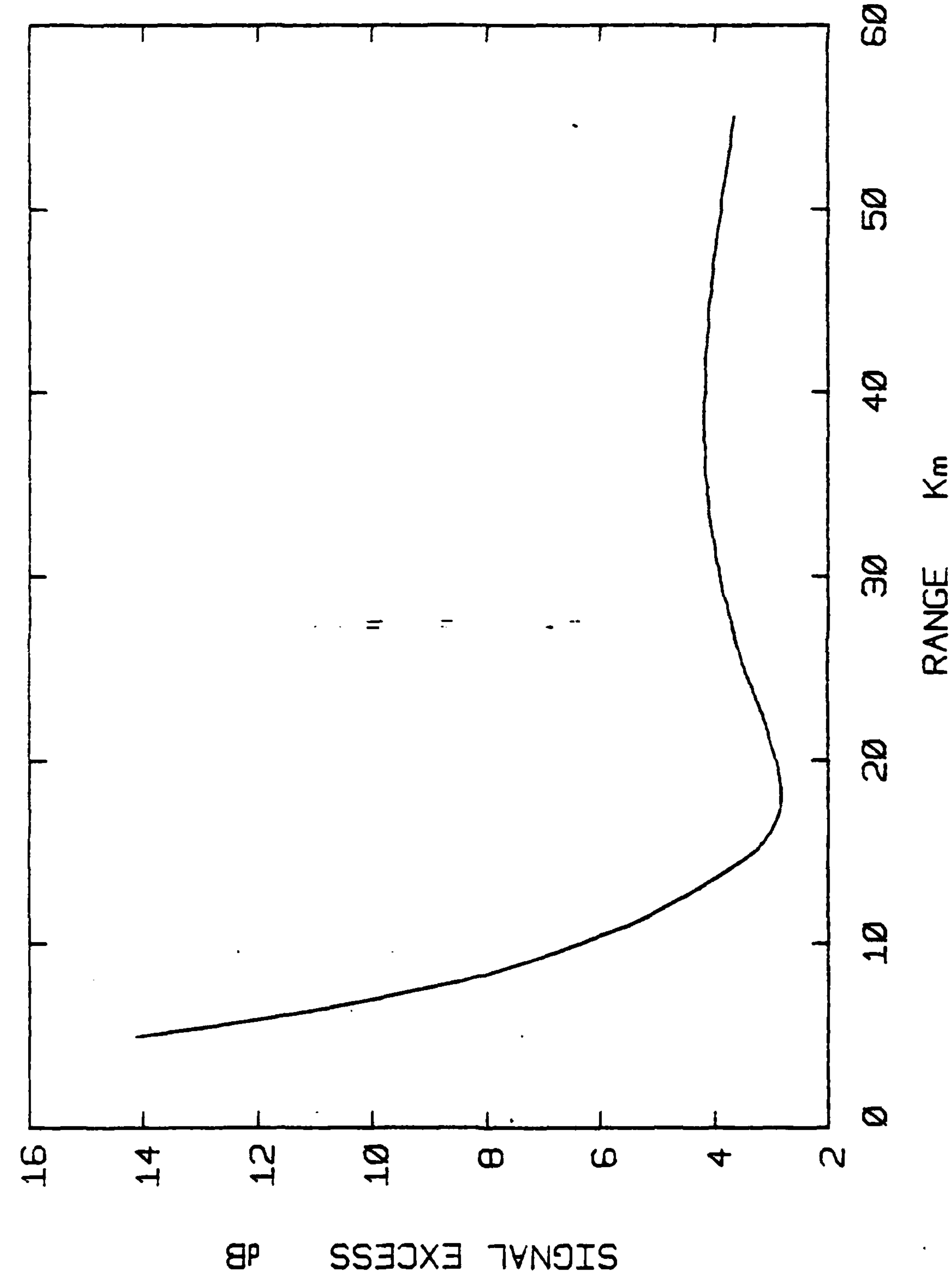

Fig. 7. Signal excess for the case shown in Fig. 6.

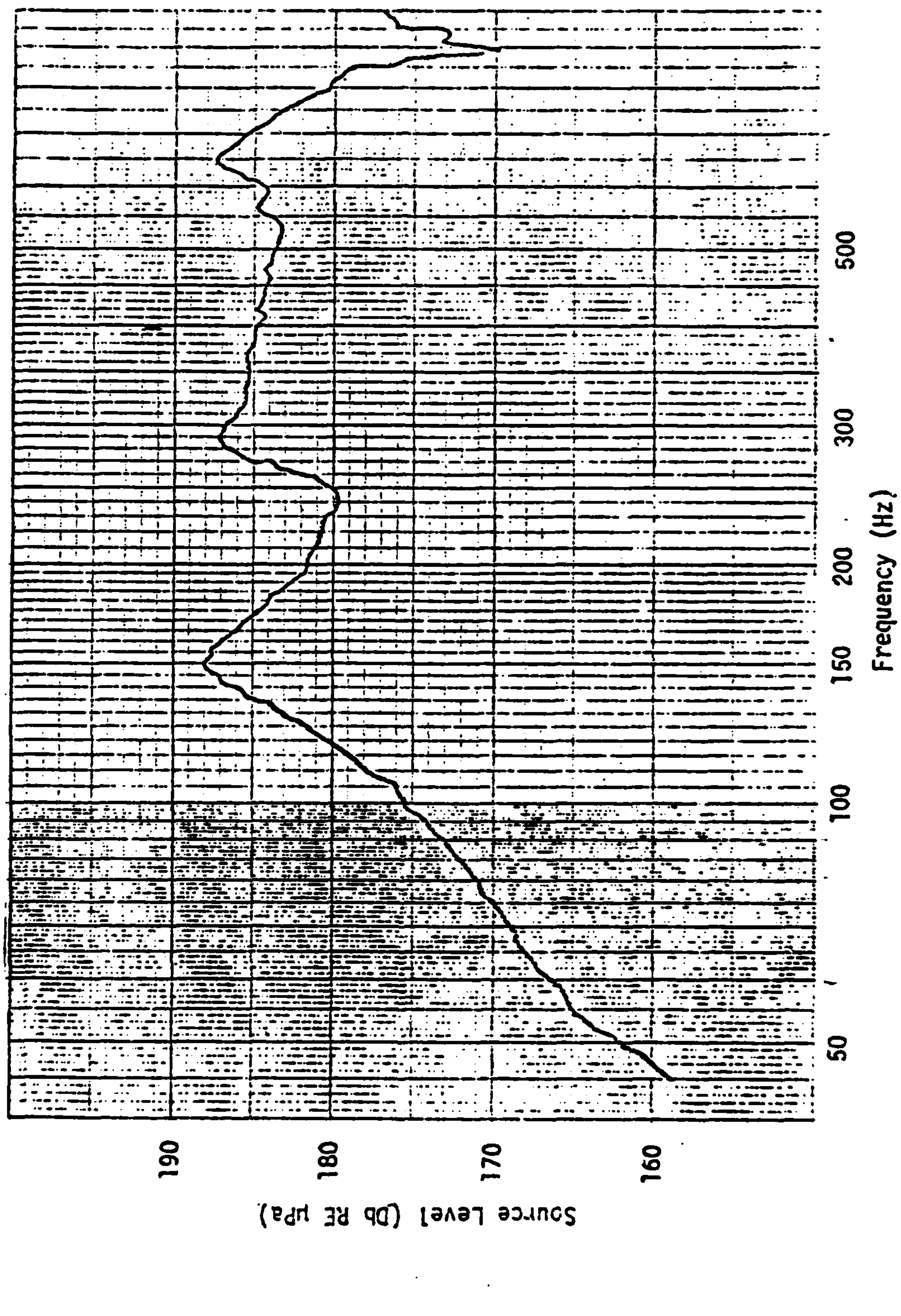

Fig. 8. Maximum source spectrum of the double HX-29 source driven in a1Hz band across frequency.

peaks. However, for the bottom bounce path (Fig. 6) the cosine reduced velocity along the line of sound eliminates this peak (see Section A).

Comparison of Fig. 4 with Fig. 5 and Fig. 6 with Fig. 7 reveals that the reduction of transmission loss as a result of reducing the range more than compensates for the loss due to doppler at the shorter ranges (except of course for the null.)

REFERENCES

[1] R.J. Urick, Sound Propagation in the Sea, Defense Advanced Research Projects Agency Publication, U.S. Government Printing Office, Washington D.C., Stock #008-051-00071-2, 1979

[2] A. Nuttall, private communication.

[3] See for example, S. Clay and H. Medwin, Acoustical Oceanography, John Wiley & Sons, New York, 1977

[4] A. Ellinthorpe and H. Freese, "Mobil Acoustic Communications System (MACS) Sea Trip Report," Naval Underwater Systems Center, New London CT., in preparation.

[5] G. Wenz, "Acoustic Ambient Noise in the Ocean", J. Acoust. Soc. Am., Vol. 34 p. 1936, 1962

[6] See for example, P. Davis and P. Rabinowitz, Numerical Integration, Blaisdell Publishing Co., Waltham, Mass. 1967.

[7] Honeywell Corporation Data Sheet TDS-110

DATE

FILMED

8 – 8